peroxide vastly exceeds that of free OHP. Spectra of the products of the oxidation of $Fe^{II}(OHP)_3$ by $HO_2^-$ are also consistent with the proposed mechanism.

An alternative mechanism would retain eq 9 (dissociative loss of OHP) and replace eq 10 and 11 with

$$Fe^{II}(OHP)_2 + H_2O_2 \rightarrow \text{"}Fe^{III}(OHP)_2(OH)\text{"} + OH \quad (13)$$

$$OH + Fe^{II}(OHP)_3 \rightarrow Fe^{III}(OHP)_3 + OH^- \quad (14)$$

where these steps would occur rapidly relative to formation of $Fe^{II}(OHP)_2$ through eq 9. This mechanism also yields the observed stoichiometry and rate law.

The rate of spontaneous loss of OHP from $Fe^{II}(OHP)_3$ in base as in eq 9 cannot be meausured directly, because of the high stability of the complex.[19] Such a measurement would provide an important test of either proposed mechanism. The substitution reaction by $CN^-$ was undertaken to provide an indirect measure of this aquation, since $CN^-$ has been shown to be an effective scavenger in such systems.[20] Our observed rate law is indeed independent of $[CN^-]$, which is consistent with a substitution reaction that proceeds by rate-limiting spontaneous loss of OHP. Since the rate constant for the $CN^-$ reaction is approximately half that for the reaction with $HO_2^-$, we have strong support for the proposed mechanisms, because each $HO_2^-$ consumes two $Fe^{II}(OHP)_3$. Thus, at this time all the data point toward a prior ligand dissociation reaction, which enables the $HO_2^-$ to find a reactive form of iron(II) in the oxidation of $Fe^{II}(OHP)_3$.

It is not surprising that $HO_2^-$ finds a pathway to oxidize $Fe^{II}(OHP)_3$ that does not involve direct outer-sphere electron transfer. The reason is that such a process would cleave the O–O bond as in

$$H_2O_2 + e^- \rightarrow OH + OH^- \quad (15)$$

Activation barriers for outer-sphere reductive cleavage have been discussed previously in the context of the $I_2^-/2I^-$ system.[21] By analogy the reduction of $H_2O_2$ could be written as having a first step

$$Fe^{II} + H_2O_2 \rightarrow Fe^{III} + HO,OH^- \quad (16)$$

and this step could be analyzed in terms of the Marcus cross relationship. An essential component of the analysis is then the hypothetical self-exchange reaction of $H_2O_2$ with $HO,OH^-$. To attain the transition state for this self-exchange reaction would require stretching the O–O bond of $H_2O_2$ by several tenths of an angstrom. Since the aqueous dissociation free energy of $H_2O_2$ is 184 kJ, the self-exchange reaction must have an enormous activation barrier. Hence, outer-sphere reduction of $H_2O_2$ is expected to occur only under rare circumstances. By contrast the barrier for $I_2^-$ is much lower, and outer-sphere reductive cleavage of $I_2^-$ is a common process. These same arguments may be applied to the second mechanism proposed for reduction of $HO_2^-$ by $Fe^{II}(OHP)_3$ in which peroxide is cleaved by $Fe^{II}(OHP)_2$ (eq 13): such a mechanism, if it occurs, must involve cleavage of peroxide after it has become coordinated to Fe(II).

**Acknowledgment.** This research was supported by the NSF (Grant CHE-8215501) and the Robert A. Welch Foundation.

**Registry No.** $Fe^{II}(OHP)_3$, 15053-63-1; $Fe^{III}(OHP)_3$, 18517-23-2; $Fe^{III}(OHP)_2(OH)$, 107890-90-4; $Fe^{II}(OHP)_2(CN)_2$, 107890-91-5; $O_2$, 7782-44-7; $HO_2^-$, 14691-59-9; $CN^-$, 57-12-5.

(19) Burgess, J.; Prince, R. H. *J. Chem. Soc.* **1965**, 4697-4705.
(20) See, for example: Mikhail, F. M.; Askami, P.; Burgess, J.; Sherry, R. *Transition Met. Chem. (Weinheim, Ger.)* **1981**, *6*, 51-54.
(21) Stanbury, D. M. *Inorg. Chem.* **1984**, *23*, 2914-2916.

Contribution from the Institut für Anorganische und Analytische Chemie, Universität Freiburg, 7800 Freiburg, FRG, and Sektion für Röntgen- und Elektronenbeugung, Universität Ulm, 7900 Ulm, FRG

# Formation of $[Pt^{2.25}]_4$-1-Methyluracil Blue through Silver(I) Oxidation of $[Pt^{2.0}]_2$ and Isolation of a Heteronuclear ($Pt_2$,$Ag_2$) Precursor

Bernhard Lippert,*[1a] Helmut Schöllhorn,[1b] and Ulf Thewalt[1b]

*Received August 19, 1986*

The oxidation of the diplatinum(II) complex (*head–head* isomer) *cis*-$[(NH_3)_2Pt(1\text{-MeU})]_2(NO_3)_2$ (1-MeU = 1-methyluracil anion, $C_5H_5N_2O_2$) to the mixed-valence-state complex $[(NH_3)_2Pt(1\text{-MeU})]_4(NO_3)_5\cdot 5H_2O$ ($Pt^{2.25}$–1-MeU blue) in the presence of $Ag^I$, $Fe^{III}$, $Ce^{IV}$, and $Cu^{II}$ has been studied. In the case of $Ag^I$, oxidation of Pt is coupled with reduction of $Ag^I$ to $Ag^0$, as shown by a combination of potentiometric titration of $Ag^I$ and visible spectroscopy. A heteronuclear complex of composition *cis*-$\{[(NH_3)_2Pt(1\text{-MeU})]_2Ag\}(NO_3)_3\cdot AgNO_3\cdot 0.5H_2O$ (**1b**), obtained on cocrystallization of the diplatinum(II) starting compound and $AgNO_3$, appears to be a direct precursor of $Pt^{2.25}$–1-MeU blue. **1b** crystallizes in space group $P\bar{1}$, with $a$ = 13.470 (4) Å, $b$ = 11.656 (5) Å, $c$ = 10.185 (3) Å, $\alpha$ = 104.89 (3)°, $\beta$ = 107.29 (2)°, $\gamma$ = 104.99 (4)°, $V$ = 1374.9 Å$^3$, and $Z$ = 1. In this compound, the dinuclear Pt compound (Pt coordination through N3 and O4) has a Ag bound via the still available O2 sites, while a second Ag links two trinuclear $Pt_2$,Ag units without being directly coordinated to the 1-MeU rings. As a result, four Ag atoms take part in a 12-membered ring, which contains also bridging nitrate groups and in addition an aqua bridge. The intramolecular Pt–Pt distance in **1b** is 2.885 (1) Å, which is between the distances observed in the diplatinum(II) starting compound (2.937 (1) Å) and in $Pt^{2.25}$–1-MeU blue (2.802 (1) Å), while the intramolecular Pt–Ag separation is 2.860 (3) Å. It is suggested that the pronounced shortening of the Pt–Pt distance in **1b** as compared to the distance in the starting compound precedes the actual electron transfer from the $Pt_2$ core to the $Ag^I$ and that oxidation of the diplatinum(II) starting compound by other transition metals may also occur via formation of heteronuclear intermediates.

## Introduction

$Ag^I$ occasionally has been applied as oxidizing agent for mono-[2] and dinuclear transition-metal complexes.[3-5] Among the latter, both Kuyper[3] and Bancroft et al.[5] have shown that $Ag^I$ can remove two electrons from dinuclear $Pt^{II}$ complexes to give diplatinum(III)

Scheme I

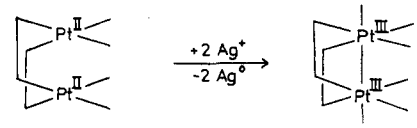


(1) (a) Universität Freiburg. (b) Universität Ulm.
(2) See, e.g.: (a) Baker, P. K.; Broadley, K.; Connelly, N. G.; Kelly, B. A.; Kitchen, M. D.; Woodward, P. *J. Chem. Soc., Dalton Trans.* **1980**, 1710. (b) Moore, D. S.; Alves, A. S.; Wilkinson, G. *J. Chem. Soc., Chem. Commun.* **1981**, 1164. (c) Werner, H.; Gotzig, J. *J. Organomet. Chem.* **1985**, *284*, 73.

0020-1669/87/1326-1736$01.50/0 

**Scheme II**

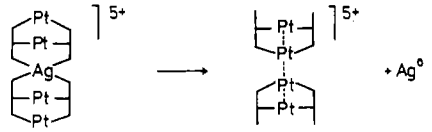

species with formation of a metal–metal single bond (Scheme I). The mechanism of this redox process has not been elucidated, but it has been suggested[3] that an addition complex between $[Pt^{II}]_2$ and $Ag^I$, possibly with a Pt–Ag bond, may be involved as an intermediate.

A while ago,[6] we reported on a 1-electron transfer (or formally 0.5-electron transfer per dinuclear unit) that took place when a pentanuclear $Pt_4$,Ag complex was warmed (Scheme II). The oxidation product, *cis*-$\{[(NH_3)_2Pt(1\text{-}MeU)]_2\}_2(NO_3)_5\cdot 5H_2O$ (1-MeU = 1-methyluracil anion, $C_5H_5N_2O_2$), is a mixed-valence-state compound (average $Pt^{2.25}$), containing formally one $Pt^{III}$ and three $Pt^{II}$ atoms. The crystal structure of this compound, obtained in an alternative way through oxidation of the $[Pt^{II}]_2$ complex with $HNO_3$–$O_2$, has been reported.[7]

In the course of our studies relating to the formation and structure of "platinum pyrimidine blues"[8] and heteronuclear derivatives,[9] we have now isolated a heteronuclear complex, *cis*-$\{[(NH_3)_2Pt(1\text{-}MeU)]_2Ag\}(NO_3)_3\cdot AgNO_3\cdot 0.5H_2O$, which appears to be a direct precursor of $Pt^{2.25}$–1-methyluracil blue. In this complex, two *cis*-$\{[(NH_3)_2Pt(1\text{-}MeU)]_2Ag\}^{3+}$ units, containing the uracil ligands in head–head arrangement and the metals coordinated via O4 (Pt), N3 (Pt), and O2 (Ag), are stacked on top of each other, very similar to the situation in $Pt^{2.25}$–1-methyluracil blue. The second $Ag^I$ (per trinuclear unit) is linked to the $Pt_2$,Ag core through water and nitrate oxygens. We suggest that the crystal structure of this complex provides a rationale for the formation of $Pt^{2.25}$–1-MeU blue in solution and thus represents an example of an isolated precursor complex of an inner-sphere electron transfer process between two different transition metals.

## Experimental Section

**Preparations.** The head–head starting dimer *cis*-$[(NH_3)_2Pt(1\text{-}MeU)]_2(NO_3)_2$ was prepared as described.[10] The preparation of the pentanuclear complex *cis*-$\{[(NH_3)_2Pt(1\text{-}MeU)]_4Ag\}(NO_3)_5\cdot 4H_2O$ (**1a**) and its crystal structure have been reported.[6] Minor products in this preparation were $Pt^{2.25}$–1-MeU blue (**2**) and *cis*-$[(NH_3)_2Pt(1\text{-}MeU)_2Ag(1\text{-}MeU)_2Pt(NH_3)_2]NO_3$ (**3**). After removal of these products and upon slow evaporation of the resulting solution, golden yellow crystals of the title compound, *cis*-$\{[(NH_3)_2Pt(1\text{-}MeU)]_2Ag\}(NO_3)_3\cdot AgNO_3\cdot 0.5H_2O$ (**1b**), were obtained.

In a slightly modified version, the head–head $[Pt^{II}]_2$ starting compound (0.25 mmol) was dissolved in water (6 mL), $AgNO_3$ (1.5 mmol, giving $c_{Ag}:c_{Pt}$ = 1:3) added, and the yellow solution allowed to slowly evaporate at room temperature. After 3 days, during which the solution became blue-green, 50 mg of a mixture of **1b** and **2** was filtered off. From the resulting solution, 100–120 mg of golden yellow crystals of **1b** were isolated prior to solidification of the sample. In both preparations, the formation of metallic Ag particles was observed. Anal. Calcd for $Pt_2Ag_2C_{10}H_{23}N_{12}O_{16.5}$: C, 10.17; H, 1.97; N, 14.23; Ag, 18.26. Found: C, 10.13; H, 2.20; N, 14.11; Ag, 18.0. Crystals of **1b** are stable in air. Prolonged storage (>1 year) at room temperature results in a change in appearance (metallic coating with golden silver luster), which is, however, restricted to the crystal surface.

**Table I.** Crystallographic Data for $[Pt_2Ag_2C_{10}H_{23}N_{12}O_{16.5}]_2$ (**1b**)

| | |
|---|---|
| fw | 2362.52 |
| space group | $P\bar{1}$ |
| $a$, Å | 13.470 (4) |
| $b$, Å | 11.656 (5) |
| $c$, Å | 10.185 (3) |
| $\alpha$, deg | 104.89 (3) |
| $\beta$, deg | 107.29 (2) |
| $\gamma$, deg | 104.99 (4) |
| $V$, Å$^3$ | 1374.9 |
| $Z$ | 1 |
| $d_{calcd}$, g cm$^{-3}$ | 2.853 |
| $d_{measd}$, g cm$^{-3}$ | 2.87 |
| cryst size, mm | 0.1, 0.1, 0.1 |
| $\mu$, cm$^{-1}$ | 111.3 |
| $\theta$ range, deg | 2–25 |
| scan mode | $\theta/2\theta$ |
| no. of measd reflecns | 9680 ($\pm h,\pm k,\pm l$) |
| no. of reflecns used in calcns | 3249 ($I > 2\sigma(I)$) |
| no. of params | 205 |
| $R$ | 0.057 (unit wts) |

Preparation of $Pt^{2.25}$–1-MeU blue (**2**) via oxidation with $Ce^{IV}$ or $Fe^{III}$ was achieved as follows: 0.1 mmol of *cis*-$[(NH_3)_2Pt(1\text{-}MeU)]_2(NO_3)_2$ (head–head) was dissolved in 10 mL of water, and 0.05 mmol of $Ce(SO_4)_2\cdot 4H_2O$ or $Fe(NO_3)_3\cdot 9H_2O$, respectively, was added (Pt:M = 4:1). The yellow solution rapidly turned turquoise-green (pH $\simeq$2), and on addition of excess $NaNO_3$ (100–400 mg), thin needles of **2** began to precipitate. After several hours at 3 °C, **2** was filtered off from the solution, washed with a small amount of ice-cold water, and dried in air. Yields were 75% (oxidation with $Ce^{IV}$) and 80% (oxidation with $Fe^{III}$). IR and UV–visible spectra and elemental analyses (C, H, N, O, Pt) confirmed the identity of **2**.

**Measurements.** UV–visible spectra were recorded on a Perkin-Elmer 555 spectrophotometer. Potentiometric measurements were carried out by using a combined Ag electrode and a Metrohm potentiometer.

**Crystallography.** The X-ray data were collected at room temperature on a Philips PW-1100 single-crystal diffractometer by using graphite-monochromated Mo K$\alpha$ radiation ($\lambda$ = 0.710 69 Å). The unit cell dimensions were calculated from 40 reflections. Crystal and structure determination data are summarized in Table I. Lp and in a later stage an empirical absorption[11] correction were applied. The positions of the metals were obtained from an $E$ map generated by the direct-methods program XMY 80.[12] Subsequent $\Delta F$ syntheses provided the positions of the non-hydrogen atoms. Hydrogens were ignored. In the course of the structure refinement it became evident that the N7-nitrate group is disordered (see Results and Discussion) and that, for reasons of charge balance, one of the other nitrates (N9) has an occupancy factor of 0.5. The metal atoms were refined with anisotropic thermal parameters; the other atoms were refined isotropically. Final atomic coordinates are given in Table II. The anisotropic thermal parameters are included in the supplementary material. The highest peak in the final difference map was 2.3 e Å$^{-3}$ (0.9 Å away from Pt1). Complex scattering factors for neutral atoms were taken from ref 13. For the calculations the SHELX program package was used.[14]

## Results and Discussion

**Formation of $[Pt_4,Ag,L_4]^{5+}$ and $[Pt_2,Ag_2,L_2]^{4+}$ and Solution Behavior.** Cocrystallization of the head–head dimer *cis*-$[(NH_3)_2PtL]_2(NO_3)_2$ (L = 1-MeU anion) with excess $AgNO_3$ ($c_{Pt}:c_{Ag}$ = 1:2 or 1:3) gave two main products, *cis*-$\{[(NH_3)_2PtL]_4Ag\}(NO_3)_5\cdot 4H_2O$ (**1a**) and *cis*-$\{[(NH_3)_2PtL]_2Ag_2\}(NO_3)_4\cdot 0.5H_2O$ (**1b**). In addition, the formation of $Pt^{2.25}$–1-MeU blue, *cis*-$[(NH_3)_2PtL]_4(NO_3)_5\cdot 5H_2O$ (**2**), metallic silver, and, occasionally, *cis*-$\{[(NH_3)_2PtL_2]_2Ag\}NO_3$ (**3**) was observed. Formation of compounds **1a** and **1b** can be rationalized as shown in equilibria 1–3. We believe that equilibrium

(3) Kuyper, J.; Vrieze, K. *Transition Met. Chem. (Weinheim, Ger.)* **1976**, *1*, 208.
(4) Piraino, P.; Bruno, G.; Nicolo, F.; Faraone, F.; Lo Schiavo, S. *Inorg. Chem.* **1985**, *24*, 4760.
(5) Bancroft, D. P.; Cotton, F. A.; Falvello, L. R.; Schwotzer, W. *Inorg. Chem.* **1986**, *25*, 763.
(6) Lippert, B.; Neugebauer, D. *Inorg. Chem.* **1982**, *21*, 451.
(7) Mascharak, P. K.; Williams, I. D.; Lippard, S. J. *J. Am. Chem. Soc.* **1984**, *106*, 6428.
(8) Lippert, B. *Inorg. Chem.* **1981**, *20*, 4326 and references cited therein.
(9) Goodgame, D. M. L.; Rollins, R. W.; Lippert, B. *Polyhedron* **1985**, *4*, 829 and references cited therein.
(10) Lippert, B.; Neugebauer, D.; Raudaschl, G. *Inorg. Chim. Acta* **1983**, *78*, 161.
(11) Walker, N.; Stuart, D. *Acta Crystallogr., Sect. A: Found. Crystallogr.* **1983**, *A39*, 158.
(12) Debardemaeker, T.; Woolfson, M. M. *Acta Crystallogr., Sect. A: Found. Crystallogr.* **1983**, *A39*, 193.
(13) (a) Cromer, D. T.; Mann, J. B. *Acta Crystallogr., Sect. A: Cryst. Phys., Diffr., Theor. Gen. Crystallogr.* **1968**, *A24*, 321. (b) Cromer, D.; Liberman, D. *J. Chem. Phys.* **1970**, *53*, 1891.
(14) Sheldrick, G. M. "SHELX, Program for Crystal Structure Determination"; University of Göttingen: Göttingen, West Germany, 1976.

$$2[Pt^{2.0}L]_2^{2+} + Ag^+ \rightleftharpoons \underset{\mathbf{1a}}{\{[Pt^{2.0}L]_4Ag\}^{5+}} \quad (1)$$

$$\underset{\mathbf{1a}}{\{[Pt^{2.0}L]_4Ag\}^{5+}} + Ag^+ \rightleftharpoons 2\underset{\mathbf{1b'}}{\{[Pt^{2.0}L]_2Ag\}^{3+}} \quad (2)$$

$$\underset{\mathbf{1b'}}{\{[Pt^{2.0}L]_2Ag\}^{3+}} + Ag^+ \rightleftharpoons \underset{\mathbf{1b}}{\{[Pt^{2.0}L]_2Ag_2\}^{4+}} \quad (3)$$

3, which describes the formation of the title compound, is relevant only in highly concentrated solution prior to crystallization.

Alternatively to coordinating to the $[Pt^{2.0}L]_2^{2+}$ unit as in **1a** and **1b'**, $Ag^+$ is also capable of substituting the Pt bound to the two L ligands via O4[15] (equilibrium 4). However, only in heated samples are significant amounts of **3** formed.

$$2[Pt^{2.0}L]_2^{2+} + Ag^+ \rightleftharpoons \underset{\mathbf{3}}{\{[Pt^{2.0}L_2]_2Ag\}^{+}} + 2[Pt^{2.0}]^{2+} \quad (4)$$

$$[Pt^{2.0}]^{2+} = cis\text{-}[(NH_3)_2Pt(OH_2)_2]^{2+}$$

Mixtures containing the head–head dimer *cis*-$[(NH_3)_2PtL]_2(NO_3)_2$ and $AgNO_3$ always became greenish blue with time, and brown-blue, dichroic crystals of $Pt^{2.25}$–1-MeU blue (**2**) formed. This process was accompanied by the appearance of shiny metal particles, frequently floating at the surface of the solution, which were unambiguously identified as being silver.[16] This finding led us[6] to conclude that it was $Ag^+$ that caused oxidation of $Pt^{2.0}$:

$$\underset{\mathbf{1a}}{\{[Pt^{2.0}L]_4Ag\}^{5+}} \rightarrow \underset{\mathbf{2}}{[Pt^{2.25}L]_4^{5+}} + Ag^0 \quad (5)$$

On the basis of the structural results presented in this paper, this redox process might also be formulated as

$$\underset{\mathbf{1b'}}{\{[Pt^{2.0}L]_2Ag\}^{3+}} \rightarrow [Pt^{2.5}L]_2^{3+} + Ag^0 \quad (6a)$$

$$[Pt^{2.5}L]_2^{3+} + [Pt^{2.0}L]_2^{2+} \rightleftharpoons \underset{\mathbf{2}}{[Pt^{2.25}L]_4^{5+}} \quad (6b)$$

The conclusions drawn from the preparative findings have now been verified in two independent experiments.

**Visible Spectroscopy.** Formation of $Pt^{2.25}$–1-MeU blue (**2**) was followed in $2.5 \times 10^{-3}$ N $HNO_3$ (Figure 1). In the absence of $Ag^+$, a faint green color (maximum around 740 nm) evolved on brief heating (2 min, 80 °C) due to formation of a small amount of **2**. If $AgNO_3$ was added, an intense absorption at 740 nm and two minor absorptions around 620 and 480 nm occurred. The spectrum obtained was in complete agreement with the spectrum of $Pt^{2.25}$–1-MeU blue prepared according to Mascharak et al.[7] The spectrum also exhibited a time dependence (fading of the green) similar to that of $Pt^{2.25}$–1-MeU blue.[17,18]

**Potentiometric Studies.** While the visible spectra indicated the involvement of $Ag^+$ in the oxidation process of the head–head $Pt^{2.0}$ dimer to $Pt^{2.25}$–1-MeU blue, they did not prove that $Ag^+$ acted stoichiometrically as oxidizing agent (as opposed to catalytically with oxygen being the ultimate oxidant). Formation of $Ag^0$, however, and its quantification clearly demonstrated that $Ag^+$ was the oxidizing agent. Solutions containing the head–head $Pt^{2.0}$ dimer and $AgNO_3$ (typically $c_{Pt}:c_{Ag}$ = 2:1) were titrated with HCl prior to and after formation of **2** and the end points determined potentiometrically with a combined Ag electrode (Figure 2). Assuming a complete oxidation of the Pt starting dimer (eq 4 or

**Table II.** Positional Parameters[a]

| atom | x | y | z |
|---|---|---|---|
| Pt1 | 0.9193 (1) | 0.0415 (1) | 0.8898 (1) |
| Pt2 | 0.7571 (1) | 0.1572 (1) | 0.8059 (1) |
| Ag1 | 0.5882 (1) | 0.2662 (2) | 0.7587 (2) |
| Ag2 | 0.5919 (2) | 0.5748 (2) | 0.7362 (3) |
| N1 | 1.032 (2) | 0.094 (2) | 0.803 (3) |
| N2 | 0.863 (2) | −0.134 (2) | 0.739 (3) |
| N3 | 0.685 (2) | 0.048 (2) | 0.588 (3) |
| N4 | 0.857 (2) | 0.296 (2) | 0.762 (2) |
| N1a | 0.836 (2) | 0.435 (2) | 1.224 (2) |
| C1a' | 0.776 (3) | 0.514 (4) | 1.280 (4) |
| C2a | 0.779 (2) | 0.341 (2) | 1.082 (3) |
| O2a' | 0.678 (2) | 0.326 (2) | 1.016 (2) |
| N3a | 0.832 (2) | 0.272 (2) | 1.021 (2) |
| C4a | 0.940 (2) | 0.291 (2) | 1.102 (2) |
| O4a' | 0.990 (2) | 0.217 (2) | 1.057 (2) |
| C5a | 1.001 (2) | 0.392 (2) | 1.244 (3) |
| C6a | 0.947 (2) | 0.462 (3) | 1.296 (3) |
| N1b' | 0.480 (2) | −0.103 (2) | 0.827 (2) |
| C1b' | 0.356 (2) | −0.143 (3) | 0.757 (3) |
| C2b | 0.545 (2) | −0.009 (3) | 0.797 (3) |
| O2b' | 0.501 (2) | 0.039 (2) | 0.717 (2) |
| N3b | 0.660 (2) | 0.018 (2) | 0.854 (2) |
| C4b | 0.703 (2) | −0.042 (2) | 0.932 (3) |
| O4b' | 0.809 (2) | −0.023 (2) | 0.977 (2) |
| C5b | 0.636 (2) | −0.134 (3) | 0.973 (3) |
| C6b | 0.524 (3) | −0.158 (3) | 0.919 (3) |
| N5 | 0.804 (2) | 0.573 (3) | 0.925 (3) |
| O1 | 0.749 (2) | 0.495 (2) | 0.797 (3) |
| O2 | 0.780 (2) | 0.673 (2) | 0.956 (3) |
| O3 | 0.886 (2) | 0.563 (2) | 1.008 (3) |
| N6 | 0.494 (3) | 0.290 (4) | 0.439 (4) |
| O4 | 0.567 (3) | 0.394 (3) | 0.454 (4) |
| O5 | 0.393 (3) | 0.258 (3) | 0.359 (4) |
| O6 | 0.532 (3) | 0.216 (4) | 0.505 (5) |
| N7* | 0.474 (4) | 0.432 (4) | 0.880 (5) |
| O7* | 0.528 (4) | 0.557 (4) | 0.953 (5) |
| O8 | 0.474 (2) | 0.391 (2) | 0.761 (2) |
| O9* | 0.432 (4) | 0.373 (4) | 0.947 (5) |
| N8 | 0.084 (3) | 0.834 (3) | 0.568 (4) |
| O10 | 0.078 (3) | 0.853 (3) | 0.688 (4) |
| O11 | 0.124 (3) | 0.759 (4) | 0.520 (4) |
| O12 | −0.001 (7) | 0.812 (8) | 0.467 (9) |
| N9* | 0.238 (4) | 1.168 (5) | 0.608 (6) |
| O13* | 0.281 (3) | 1.210 (4) | 0.562 (4) |
| O14* | 0.239 (6) | 1.197 (6) | 0.740 (8) |
| O15* | 0.159 (8) | 1.072 (9) | 0.54 (1) |

[a] Atoms marked with an asterisk were refined with fixed occupancy factors of 0.5.

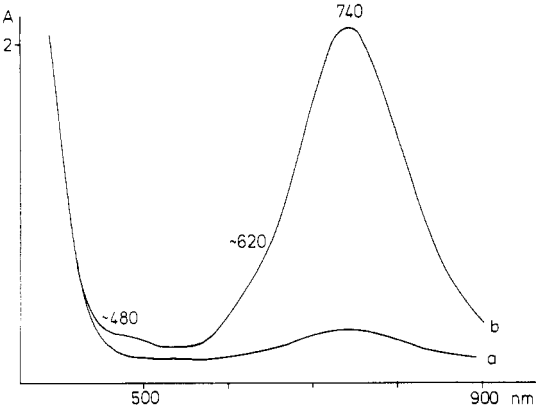


**Figure 1.** Visible spectra of samples of head–head $[Pt^{2.0}]_2$ (0.1 mmol in 2 mL of 0.005 N $HNO_3$): (a) after 2 min at 80 °C; (b) with added $AgNO_3$ (0.1 mmol), after 2 min at 80 °C. Samples were diluted 1:1 with $H_2O$ prior to spectra recording. The absorbing species is $Pt^{2.25}$–1-MeU blue.

(15) Thewalt, U.; Neugebauer, D.; Lippert, B. *Inorg. Chem.* **1984**, *23*, 1713.
(16) The sample was brought to dryness, repeatedly treated with water to remove any soluble material, and centrifuged each time. The final wash was free of $Ag^+$. The grayish, metallic residue was dissolved in concentrated $HNO_3$, the solution heated to remove excess $HNO_3$, and the residue redissolved in water and analyzed for $Ag^+$.
(17) The 740-nm band decays with a half-life of ca. 1.5 h in 0.01 N $HNO_3$ and of ca. 2 h in 0.1 N $HNO_3$ (concentrations of $Pt^{2.25}$–1-MeU blue $1.8 \times 10^{-4}$ and $2.0 \times 10^{-4}$ mol $L^{-1}$, respectively).
(18) We note some discrepancies between the visible spectrum of $Pt^{2.25}$–1-MeU blue prepared by us and the data reported in ref 7: According to our results, **2** absorbs at 740 nm ($\epsilon \approx 8000$ $M^{-1}$ $cm^{-1}$), 620 nm (estimated $\epsilon$ = 800–1000 $M^{-1}$ $cm^{-1}$), and 480 nm ($\epsilon \approx 250$ $M^{-1}$ $cm^{-1}$ in 0.1 N $HNO_3$ ($\epsilon$ values calculated per $Pt_4$ unit). Since it takes time until **2** is completely dissolved (sample *not* heated), yet **2** decomposes in solution (cf. ref 17), the $\epsilon$ values should actually even be somewhat higher.

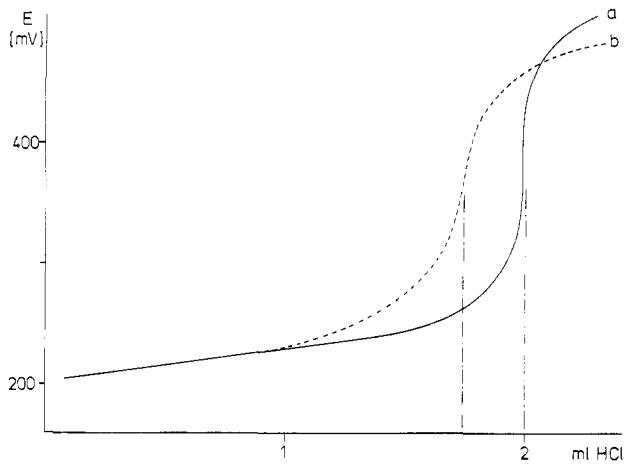


**Figure 2.** Potentiometric titration curves (0.05 N HCl): (a) $AgNO_3$ (0.1 mmol in 5.5 mL of diluted $HNO_3$, pH 2.3); (b) aged mixture of head–head $[Pt^{2.0}]_2$ and $AgNO_3$ (0.1 mmol each). The aged solution was prepared by slow evaporation (5 days, 22 °C) of the Pt–Ag mixture (in 3 mL of diluted $HNO_3$, pH 2.2) and subsequent dilution to 5.5 mL total volume (precipitated **2** redissolved with blue-green color). The titration curve of a freshly prepared mixture of $[Pt^{2.0}]_2$ and $AgNO_3$ (0.1 mmol each) is virtually identical with that of pure $AgNO_3$ (a).

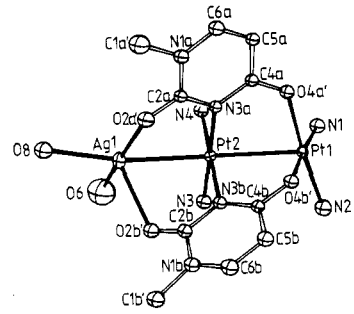


**Figure 3.** View of the trinuclear $Pt_2$,Ag cation with atom numbering.

5), 1 $Ag^+$ should be consumed per 4 $Pt^{2.0}$. Under our experimental conditions (0.1 mmol of $Pt^{2.0}$ dimer, 0.1 mmol of $AgNO_3$), 0.05 mmol of $AgNO_3$ would be required to fully oxidize the $Pt^{2.0}$ dimer to $Pt^{2.25}$–1-MeU blue. Depending on the reaction conditions, up to 25% of the $AgNO_3$ was converted into $Ag^0$.[19] The data obtained from the titration experiments correlated excellently with the results from the visible spectra concerning the concentration of $Pt^{2.25}$–1-MeU blue.[20]

**Effects of Other Metals.** Oxidation of the head–head dimer *cis*-$[(NH_3)_2PtL]_2(NO_3)_2$ to $Pt^{2.25}$–1-MeU blue occurred instantaneously when $Ce^{4+}$ or $Fe^{3+}$ was used as oxidizing agent (Pt:M = 4:1). Addition of excess $NaNO_3$ to the resulting blue-green solution precipitated $Pt^{2.25}$–1-MeU blue in high yield (cf. Experimental Section). The effect of $Cu^{2+}$ on the diplatinum(II) compound was also studied: Unlike with $Ce^{4+}$ and $Fe^{3+}$, no fast reaction was observed. Samples containing 0.05 mmol of the $[Pt^{2.0}L]_2^{2+}$ complex in 2 mL of 0.01 M $HNO_3$ were kept at room temperature in the dark (a) in air, (b) together with 0.05 mmol of $Cu(NO_3)_2$ in air, and (c) with 0.05 mmol of $Cu(NO_3)_2$ under nitrogen. Within several days, during which the volumes of the three samples had been kept constant, a precipitate of $Pt^{2.25}$–1-MeU blue had formed in sample b only. After appropriate dilution of the samples (precipitate in (b) redissolved), visible spectra were recorded. The relative intensities of the 720-nm absorptions were 1:2.6:9.2 for samples c, a, and b, respectively. This finding strongly suggests that both $Cu^{2+}$ *and* oxygen are necessary in order to accomplish oxidation of the diplatinum(II) species, which may indicate a catalytic role of $Cu^{2+}$ in the oxidation process (cf. the scheme in the supplementary material).

Finally, we note that addition of *cis*-$[(NH_3)_2Pt(OH_2)_2](NO_3)_2$ or $[Pt(OH_2)_4](NO_3)_2$ to aqueous solutions of the head–head dimer also leads to formation of $Pt^{2.25}$–1-MeU blue. However, because of the fairly acidic conditions, the role of added Pt species in the oxidation process as opposed to that of the acid $HNO_3$ is unclear at present.

**Crystal Structure of *cis*-{$[(NH_3)_2Pt(1\text{-MeU})]_2Ag$}$(NO_3)_3$·$AgNO_3$·$H_2O$ (1b).** Figure 3 gives a view of the $Pt_2$,Ag fragment of compound **1b** that contains the three metals (Pt1, Pt2, Ag1) bound to the 1-MeU ligands. Selected interatomic distances and angles are given in Table III. The 1-MeU ligands provide coordination for three metals simultaneously, through N3 and O4 for the two Pt atoms, and through O2 for Ag1. The coordination spheres of the two platinum atoms are square planar, with Pt2 well within the plane yet Pt1 slightly (0.08 Å) out of it, directed toward Pt2. The two platinum planes are tilted by 30°. Pt–N and Pt–O distances are normal.

The four oxygens around Ag1 form a strongly distorted tetrahedron with several of the angles close to 90°. Ag1–O distances vary between 2.33 (4) and 2.47 (2) Å and are thus similar to those of related mixed-Pt,Ag complexes of 1-methyluracil and 1-

**Table III.** Selected Interatomic Distances (Å) and Angles (deg) of Metal Coordination Spheres

| | | | |
|---|---|---|---|
| Pt1–Pt1* | 3.164 (1) | Pt1–Pt2 | 2.885 (1) |
| Pt2–Ag1 | 2.860 (3) | Pt1–N1 | 2.02 (3) |
| Pt1–N2 | 2.01 (2) | Pt1–O4a' | 2.06 (1) |
| Pt1–O4b' | 2.02 (2) | Pt2–N3 | 2.03 (2) |
| Pt2–N4 | 2.06 (2) | Pt2–N3a | 2.02 (2) |
| Pt2–N3b | 2.06 (2) | Ag1–O2a' | 2.36 (2) |
| Ag1–O2b' | 2.47 (2) | Ag1–O6 | 2.33 (4) |
| Ag1–O8 | 2.38 (2) | Ag2–O1 | 2.51 (3) |
| Ag2–O2 | 2.56 (2) | Ag2–O5* | 2.38 (2) |
| Ag2–O8 | 2.43 (2) | | |
| Pt1*–Pt1–Pt2 | 155 (1) | Ag1–Pt2–N3b | 91 (1) |
| Pt1*–Pt1–N1 | 92 (1) | N3–Pt2–N4 | 90 (1) |
| Pt1*–Pt1–N2 | 89 (1) | N3–Pt2–N3a | 178 (1) |
| Pt1*–Pt1–O4a' | 86 (1) | N3–Pt2–N3b | 91 (1) |
| Pt1*–Pt1–O4b' | 84 (1) | N4–Pt2–N3a | 98 (1) |
| Pt2–Pt1–N1 | 107 (1) | N4–Pt2–N3b | 179 (1) |
| Pt2–Pt1–N2 | 108 (1) | N3a–Pt2–N3b | 91 (1) |
| Pt2–Pt1–O4a' | 78 (1) | Pt2–Ag1–O6 | 99 (1) |
| Pt2–Pt1–O4b' | 77 (1) | Pt2–Ag1–O8 | 169 (1) |
| N1–Pt1–N2 | 88 (1) | Pt2–Ag1–O2a' | 73 (1) |
| N1–Pt1–O4a' | 91 (1) | Pt2–Ag1–O2b' | 71 (1) |
| N1–Pt1–O4b' | 176 (1) | O6–Ag1–O8 | 89 (1) |
| N2–Pt1–O4a' | 174 (1) | O6–Ag1–O2a' | 170 (1) |
| N2–Pt1–O4b' | 89 (1) | O6–Ag1–O2b' | 90 (1) |
| O4a'–Pt1–O4b' | 92 (1) | O8–Ag1–O2a' | 98 (1) |
| Pt1–Pt2–Ag1 | 171 (1) | O8–Ag1–O2b' | 117 (1) |
| Pt1–Pt2–N3 | 97 (1) | O2a'–Ag1–O2b' | 94 (1) |
| Pt1–Pt2–N4 | 96 (1) | O1–Ag2–O2 | 50 (1) |
| Pt1–Pt2–N3a | 84 (1) | O1–Ag2–O5* | 120 (1) |
| Pt1–Pt2–N3b | 83 (1) | O1–Ag2–O8 | 89 (1) |
| Ag1–Pt2–N3 | 88 (1) | O2–Ag2–O5* | 99 (1) |
| Ag1–Pt2–N4 | 90 (1) | O2–Ag2–O8 | 109 (1) |
| Ag1–Pt2–N3a | 91 (1) | O5*–Ag2–O8 | 149 (1) |

**Table IV.** Comparison of Intermetallic Distances in **1b** and Related Compounds (Å)

| compd | $Pt–Pt_{intra}$ | $Pt–Pt_{inter}$ | Pt–Ag | ref |
|---|---|---|---|---|
| $\{[Pt^{2.0}L]_4Ag\}^{5+}$ (**1a**) | 2.949 (2) | 3.246 (2) | 2.787 (1) | 6 |
| $[Pt^{2.0}L]_2^{2+}$ | 2.937 (1) | *a* | | 10 |
| $\{[Pt^{2.0}L]_2Ag_2\}^{4+}$ (**1b**) | 2.885 (1) | 3.164 (1) | 2.860 (3) | *b* |
| $[Pt^{2.25}L]_4^{5+}$ (**2**) | 2.802 (1)[c] | 2.865 (1) | | 7 |

[a] Packing of dimer units different. [b] This work. [c] Average value from 2.810 (1) and 2.793 (1) Å.

(19) The yield of **2** could be raised well above 50% when solutions of the head–head $Pt^{2.0}$ dimer and $AgNO_3$ (Pt:Ag = 4:1, 0.01 N $HNO_3$) were allowed to evaporate to dryness. Poorly soluble **2**, usually contaminated with $Ag^0$, was filtered off after water had been added, and the soluble part again allowed to evaporate.

(20) For example, for the sample given in Figure 2 (reduced $Ag^+$ content), we calculate a 25% yield of **2** according to eq 4 or 5. The intensity of the 740-nm band in the visible spectrum of the same sample, taken immediately after the precipitated blue was dissolved, indicates that ca. 22% of **2** is formed.

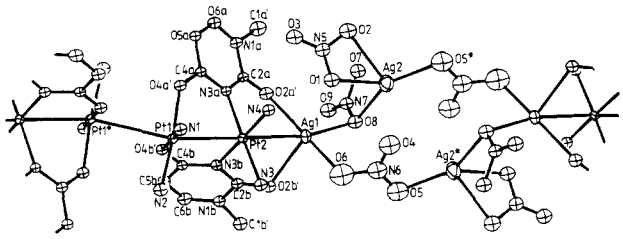

**Figure 4.** Extended view of the cation of the title compound, indicating the stacking between neighboring $Pt_2$,Ag units (left) and bridging via Ag2 and Ag2* (right). The ionic nitrate groups are omitted for clarity; the bridging nitrate (N7) and its symmetry-related counterpart (N7*) have occupancies of only 0.5 (cf. text). Ag2* is symmetry-related to Ag2.

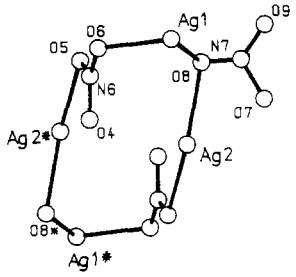

**Figure 5.** Twelve-membered ring involving four Ag atoms, three nitrates, and one $H_2O$. The drawing is idealized in that the disorder between O8 from nitrate N7 and O8* from water is not considered (cf. text).

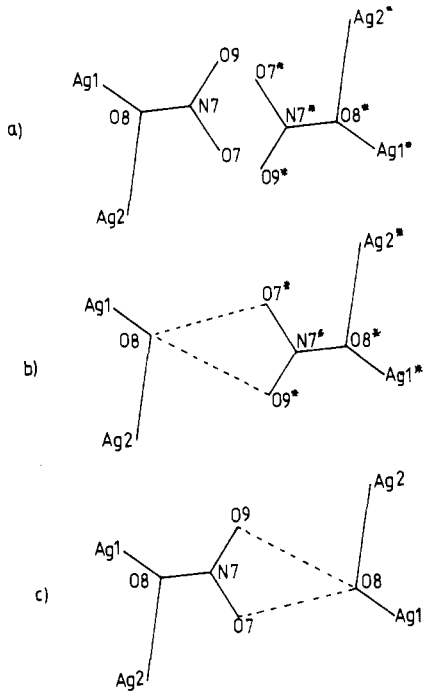

**Figure 6.** Schematic description of hydrogen bonding between strings of $Pt_2$,$Ag_2$ units and resulting disorder between nitrate and $OH_2$: (a) arrangement according to electron density map; (b, c) "resolved" arrangements, assuming disorder between two possible distributions.

methylthymine[21] as well as homonuclear Ag complexes of these or related ligands.[22]

The intermetallic distances within the trinuclear cation of **1b** differ from that of the pentanuclear $Pt_4$,Ag,$L_4$ complex **1a** in that the Pt–Pt separation in **1b** is significantly shorter ($29\sigma$),[23] while the Ag–Pt separation is longer ($23\sigma$) in **1b** (Table IV). The sums of both distances in the two compounds are approximately the same, however. As far as the Pt1–Pt2 distance is concerned, it is also significantly shorter in **1b** than in the $[Pt^{2.0}L]_2^{2+}$ starting complex ($37\sigma$) yet still considerably longer ($59\sigma$) than in $Pt^{2.25}$–1-MeU blue. The shortening of the Pt–Pt separation on Ag binding to O2 has some precedence in the tetranuclear $Pt_2$,$Ag_2$,$L_2$ complex with head–tail orientation of the two 1-MeU ligands.[15] There, the Pt–Pt separation decreases from 2.954 (2) to 2.892 (1) Å, corresponding to $28\sigma$.

Figure 4 provides an extended view of the crystal structure of **1b**. Trinuclear $Pt_2$,Ag1 units are stacked with Pt1 and Pt1* coordination planes facing each other, very much as in the $Pt_4$,Ag,$L_4$ complex **1a** and in the $Pt^{2.25}$–1-MeU blue **2**. The intermolecular Pt1–Pt1* distance is 3.164 (1) Å, which compares with 3.246 (2) Å in **1a** and 2.865 (1) Å in **2**. Again, there is a marked shortening of the Pt–Pt* distance ($36\sigma$) in **1b** as compared to that in **1a**, but clearly the Pt–Pt* separation in **1b** is still much longer than in **2**.

The role of the second Ag ion in **1b** (Ag2), which is not coordinated to the 1-MeU ring, is to link pairs of $Pt_2$,Ag,$L_2$ cations. Oxygens O5 and O6 of one nitrate are bridging Ag1 of one cation with Ag2* of the adjacent one. A second bridge between Ag1 and Ag2 is through a single oxygen (O8) of another nitrate ion and a water oxygen, respectively (cf. discussion below). As a result of this arrangement, a 12-membered ring is formed (Figure 5), which consists of four Ag ions, two O–N–O bridges (bidentate nitrate), and two single oxygens (O8 and O8*). Formation of a rather similar 12-membered ring, containing also four silver atoms, two bidentate bridging nitrates, and two aqua bridges, has recently been observed by us with the heteronuclear, mixed-nucleobase complex *cis*-$[(NH_3)_2Pt(1\text{-}MeC)(1\text{-}MeU)Ag(OH_2)](NO_3)_2 \cdot AgNO_3 \cdot 2.5H_2O$ (with 1-MeC = 1-methylcytosine).[24] Distances between the Ag ions in **1b**, which are 3.651 Å (Ag1–Ag2), 4.323 Å (Ag2–Ag2*), and 5.881 Å (Ag1–Ag2*), are too long for any direct metal–metal interaction.

The stacked $Pt_2$,Ag1 units, which are linked through Ag2 and Ag2*, thus form infinite strings. Parallel strings are connected via hydrogen bonds, as indicated in Figure 6. Figure 6 gives, at the same time, our interpretation of the above-mentioned disorder of nitrate and water oxygens (O8 and O8*) in the 12-membered ring: $\Delta F$ maps and the refinement yielded an arrangement in which the N7 nitrate group and the symmetry ($\bar{1}$)-related N7* group are unrealistically close to each other (Figure 6a). If one assumes, however, that this electron density distribution is due to a superposition of two (symmetrically equivalent) arrangements as shown in Figure 6b,c, each consisting of one nitrate plus one water molecule hydrogen bonded to each other, and further that these arrangements alternate randomly from one unit cell to the next one, one arrives at a reasonable picture. Although aqua groups bridging two metal ions are rare,[24] this interpretation is supported by the similarity with the other 12-membered ring recently observed by us in a related system.[21c] There, the bridging aqua ligands, which are not disordered, are involved in hydrogen bonding with nitrate oxygens, very similarly, as indicated in Figure 6b,c. An alternative description of this situation as hydrogen bonding between a bridging hydroxo group and $HNO_3$ appears not to be justified, considering the isolation of both compounds from solutions of pH 4–5. Our interpretation of half-occupancies of nitrate N7 and water O8 requires, for charge balance reasons, one of the other nitrate positions to be only partly occupied as well. Judging from the temperature factors, we assume that the N9 nitrate is the most likely candidate (and treat it in the final refinement with half-occupancy). There is a short contact of 2.67 Å between O8 and O13 ($x, -1 + y, z$) which can be interpreted as a O8–H···O13 hydrogen bond. Interpretation of O8 as a water molecule rather than a hydroxo group appears

(21) (a) Schöllhorn, H.; Thewalt, U.; Lippert, B. *J. Chem. Soc., Chem. Commun.* **1984**, 769. (b) Lippert, B.; Neugebauer, D. *Inorg. Chim. Acta* **1980**, *46*, 171. (c) Schöllhorn, H.; Thewalt, U.; Lippert, B. *Inorg. Chim. Acta* **1987**, *135*, 155. (d) Reference 14.

(22) (a) Perron, J.; Beauchamp, A. L. *Inorg. Chem.* **1984**, *23*, 2853. (b) Perron, J.; Beauchamp, A. L. *Can. J. Chem.* **1984**, *62*, 1287. (c) Guay, F.; Beauchamp, A. L. *J. Am. Chem. Soc.* **1979**, *101*, 6260.

(23) $\sigma$ is defined as $\sigma = (\sigma_1^2 + \sigma_2^2)^{1/2}$ with $\sigma_1$ and $\sigma_2$ being the errors in bond lengths compared.

(24) Wells, A. F. *Structural Inorganic Chemistry*; Clarendon: Oxford, England, 1984; pp 677, 688.

**Scheme III**

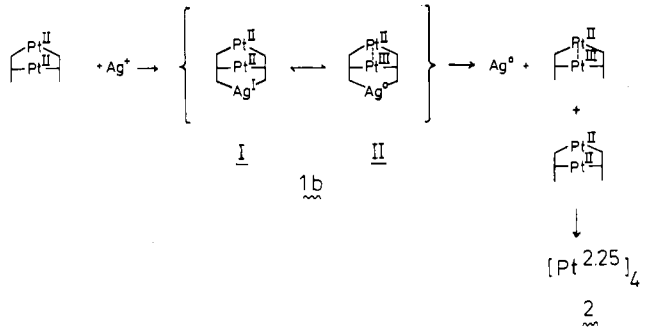

on this basis also more likely. Although we cannot fully exclude possible alternative descriptions of the disorder in this structure, we are reasonably positive that **1b** should be formulated as *cis*-$\{[(NH_3)_2Pt(1\text{-}MeU)]_2Ag_2(NO_3)_{2.5}(OH_2)_{0.5}\}(NO_3)_{1.5}$.

**$Pt_2$,Ag,$L_2$ as a Precursor Complex.** We have previously discussed changes in intramolecular Pt–Pt separations in dinuclear uracilato- or thyminato-bridged complexes in terms of effects of tilt angles between the Pt planes, of torsional angles about the Pt–Pt vectors, and of "manipulations" (metal coordination, H bonding) of the available O2 oxygens.[25] Considering the results of the structure determination of **1b** *and* its solution behavior, it is tempting to also use electronic arguments and to postulate that **1b** (and its equivalent in solution, **1b'**, respectively) is a direct precursor of $Pt^{2.25}$–1-MeU blue. The substantial shortening of Pt–Pt in **1b** on Ag binding (almost halfway between the distance in the $[Pt^{2.0}]_2$ starting compound and that in $Pt^{2.25}$–1-MeU blue) suggests that one electron of the HOMO of the $Pt_2$ core is already "on its way" to $Ag^+$; hence, a situation is approached that might be described by the resonance structures I and II given in Scheme III. On the basis of redox potentials ($E°_{Pt(2.0)/Pt(2.25)}$ = 780 mV,[26] $E°_{Ag(0)/Ag(I)}$ = 810 mV) electron transfer to Ag(I) certainly is not unexpected. Attempts to monitor the decay of **1b** rather than the formation of **2** spectroscopically in solution, e.g. via a CT band of **1b**, were unsuccessful, because no such band could be identified between 300 and 900 nm.[27] A low complex stability of **1b** and/or the need of higher concentrations (to accomplish dimer-to-dimer association) might account for this failure. Studies are under way to find out whether the results reported here can be substantiated for the interaction of dinuclear Pt complexes with other redox-active transition metals.

**Acknowledgment.** This work has been supported by the Deutsche Forschungsgemeinschaft and the Fonds der Chemischen Industrie. We thank I. Dettinger for experimental assistance.

**Registry No.** **1b**, 107846-63-9; **2**, 92220-63-8; *cis*-$[(NH_3)_2Pt(1\text{-}MeU)]_2(NO_3)_2$, 85886-74-4; $AgNO_3$, 7761-88-8; $Ce(SO_4)_2$, 13590-82-4; $Fe(NO_3)_3$, 10421-48-4; $Cu^{2+}$, 15158-11-9.

**Supplementary Material Available:** Listings of positional parameters, distances and angles of 1-MeU ligands and nitrates, possible H-bonding interactions, and conformational parameters and a proposed reaction scheme between $[Pt^{2.0}]_2$ and $Cu^{II}$–$O_2$ (5 pages); a listing of observed and calculated structure factors (14 pages). Ordering information is given on any current masthead page.

(25) Schöllhorn, H.; Thewalt, U.; Lippert, B. *Inorg. Chim. Acta* **1984**, *93*, 19.

(26) Micklitz, W.; Riede, J.; Müller, G.; Lippert, B., to be submitted for publication in *Inorg. Chem.*

(27) On the basis of the color of **1b** in the solid state (golden yellow, tint toward orange as opposed to pale yellow for $[Pt^{2.0}]_2$) one might expect an absorption in the 420–490-nm range.

Contribution from the Chemical Physics Group,
Tata Institute of Fundamental Research, Colaba, Bombay 400 005, India

# Electronic Structure of Hemin Chloride in Pyridine and Pyridine–Chloroform Solution: Proton NMR Study

L. B. Dugad, O. K. Medhi,† and Samaresh Mitra*

*Received February 12, 1986*

Variable-temperature $^1H$ NMR measurements at 500 MHz on (protoporphyrinato)iron(III) chloride (hemin chloride) in pure dry pyridine and a pyridine–chloroform mixture are reported. In freshly prepared solution the autoreduction of the ferric ion in hemin chloride is minimal, and only two iron(III) complexes are generally observed. The high-spin methyl proton resonances in the 50–60 ppm range are believed to be associated with six-coordinated (pyridine)hemin chloride while the low-spin methyl resonances in the 15–25 ppm range refer to the bis(pyridine)ferric protoporphyrin complex. The temperature dependence of the proton resonances conform reasonably well to the spin assignments. Addition of chloroform to this hemin–pyridine solution slowly decreases the concentration of the high-spin complex, which finally disappears at a large excess of chloroform. The "low-spin" complex with methyl resonances in the 15–25 ppm range in the pyridine–chloroform solution shows anomalous temperature dependence, which has been satisfactorily interpreted quantitatively on a thermal spin equilibrium between $S = {}^5/_2$ and $S = {}^1/_2$.

## Introduction

The protein control of the axial ligation mode of the heme group in hemoproteins has resulted in a multiplicity of functions for the hemoproteins, such as oxygen transport in hemoglobin, electron transport in cytochrome *c*, and oxygen redox chemistry in peroxidases.[1,2] The ability to perform such diverse functions has been attributed to the easy accessibility of different oxidation and spin states of the iron in the complexed state.[3,4] The nature of the axial ligands and their reactivity toward binding iron in heme play an important role in stabilizing various oxidation and spin states.

Investigations of structure and structure-related electronic properties of the heme prosthetic group in hemoproteins and model systems have provided considerable insight into the biochemical functions of these macromolecules. The study of ligand-exchange reactions and concomitant structural changes has in particular attracted considerable attention. Such studies can be effectively

† Permanent address: Chemistry Department, Gauhati University, Guwahati 781 014, India.

(1) Smith, K. M. *Acc. Chem. Res.* **1979**, *12*, 374.
(2) Taylor, T. G. *Acc. Chem. Res.* **1981**, *14*, 102.
(3) Reed, C. A. *Met. Ions Biol. Syst.* **1978**, *7*, 277.
(4) Scheidt, W. R.; Reed, C. A. *Chem. Rev.* **1981**, *81*, 543.

0020-1669/87/1326-1741$01.50/0 